

# Morphological study on three kinds of two-dimensional spherulites of poly(butylene terephthalate) (PBT)

Taiyo Yoshioka<sup>a</sup>, Takashi Fujimura<sup>b</sup>, Norio Manabe<sup>c</sup>, Yoshimitsu Yokota<sup>c</sup>, Masaki Tsuji<sup>b,\*</sup>

<sup>a</sup> Biomaterials Center, National Institute for Materials Science, Namiki Site 1-1, Namiki, Tsukuba, Ibaraki 305-0044, Japan

<sup>b</sup> Institute for Chemical Research, Kyoto University, Uji, Kyoto-fu 611-0011, Japan

<sup>c</sup> Research and Evaluation Center, Sumitomo Wiring Systems Co., Ltd, 1820 Nakanoike, Mikkaichi-cho, Suzuka, Mie-ken 513-8631, Japan

Received 19 January 2007; received in revised form 4 July 2007; accepted 16 July 2007

Available online 20 July 2007

## Abstract

Three kinds of thin film specimens, each of which containing one of the three types of two-dimensional poly(butylene terephthalate) (PBT) spherulites (i: usual-positive type, ii: usual-negative type, and iii: unusual type), were prepared and studied mainly by transmission electron microscopy. It was confirmed that all these kinds of spherulites are made up of only the  $\alpha$ -modification crystals, and the growth directions for usual-positive type, usual-negative type, and unusual type are the  $[010]^*$ ,  $[1\bar{1}1]^*$ , and  $[2\bar{1}0]^*$  directions in the reciprocal lattice, respectively. Furthermore, the arrangement of unit cell in each type of the spherulites was determined. The relationships between the arrangements of unit cell and the types of each resulting spherulite are discussed.

© 2007 Elsevier Ltd. All rights reserved.

**Keywords:** Poly(butylene terephthalate) (PBT); Spherulite; Polymer crystallization

## 1. Introduction

Poly(butylene terephthalate) (PBT) is one of the aromatic polyesters, and is well known as an excellent material in the industrial field which needs engineering thermoplastics. PBT has lower melting point, lower glass-transition temperature, a higher crystallization rate, and a lower value of maximum attainable crystallinity than poly(ethylene terephthalate) (PET) [1,2]. Two reversible  $\alpha$ - and  $\beta$ -modification of triclinic crystal system were reported for the relaxed and stressed PBTs, respectively [3–6].

It was also reported for PBT that three different types of spherulites (i: usual-positive type, ii: usual-negative type, and iii: unusual type in which the Maltese cross pattern does not coincide in direction with the crossed polars) are formed in thin films under static condition, depending on the crystallization conditions [7–9]. In isothermal melt-crystallization,

when crystallization temperature is above 200 °C the resulting spherulites are of “usual-positive type” and when below 200 °C the resulting ones are of “unusual type” [7]. In solution-cast crystallization, when crystallization rate is adequately low the resulting spherulites are of “usual-negative type” and when adequately high the resulting ones are of “unusual type” [8].

Actually, however, in isothermal melt-crystallization it seemed difficult to obtain the well-defined usual-positive type. Recently, Lorenzo and Righetti [9] investigated three crystallization temperatures (194 °C, 204 °C and 214 °C) in the vicinity of this border temperature (200 °C) in isothermal melt-crystallization. According to them, at 194 °C the dominant type of spherulite was unusual type as same as the one reported by Stein and Misra [7]. The dominant type, however, changed to mixed type at 204 °C which has an eight-arm cross due to superposition of extinction patterns at 0° and 45°, and at 214 °C the spherulitic pattern was lost or not well defined. Stein and Misra [7] also mentioned that the spherulites formed at 200 °C did not show a clearly defined Maltese cross pattern, although a well-defined light-scattering pattern characterized as the one for usual spherulite was obtained. Roche et al.

\* Corresponding author. Tel.: +81 774 38 3061; fax: +81 774 38 3069.

E-mail address: [tsujimas@scl.kyoto-u.ac.jp](mailto:tsujimas@scl.kyoto-u.ac.jp) (M. Tsuji).

investigated by transmission electron microscopy (TEM) that the growth direction (namely, radius direction) of usual-negative type spherulite is the  $[\bar{2}10]^*$  direction, and the one of unusual type spherulites is  $[\bar{1}11]^*$  [8]. In addition to the growth direction of spherulite, the growth direction of the single crystal grown in a melt-crystallized thin film of random block copolymers of PBT and poly(tetramethylene ether glycol) was also investigated by TEM and was determined to be  $[\bar{2}10]^*$  [10,11].

The major objective of this study is to clarify structural origins of three types of PBT spherulites, each of which determining the optical property of the corresponding PBT spherulite. In our study, the growth directions of three types of spherulites were determined and each disagreed with the directions proposed by Roche et al. Furthermore, the arrangement of unit cells in a lamella for each type of spherulites was determined, and the relation between the arrangement and the optical property of spherulite is discussed.

## 2. Experimental

### 2.1. Film specimen preparation

#### 2.1.1. Melt-crystallized film specimen

PBT (molar mass:  $M_n = 5600$  g/mol,  $M_w = 26,000$  g/mol) was purchased from Polyplastics Co., Ltd. The 1.0 wt% and 0.1 wt% solutions of PBT in 1,1,1,3,3,3-hexafluoro-2-propanol (HFIP) were prepared for observations by polarizing optical microscopy (POM) and TEM, respectively. In preparing film specimens for such observations, a solution was dropped and spread on a glass slide, which had been coated with vapor-deposited carbon in advance to obtain uniform spreading of the solution. After evaporation of the solvent, the resulting thin film of PBT on the glass slide was covered with another glass slide which had also been coated with vapor-deposited carbon in advance, and then the film sandwiched between two glass slides was melted on the hot plate thermostated at 260 °C. After melting of the film for 10 min, this “sandwich” was transferred from the hot plate (260 °C) to another one thermostated at a desired crystallization temperature (68 °C, 95 °C, 163 °C and 210 °C) as quickly as possible (<1 s), and the film was isothermally crystallized for a proper crystallization time. These four crystallization temperatures were chosen because each temperature corresponds to the melting point of calibration substance: azobenzene (68 °C), benzil (95 °C), benzanilide (163 °C) and dicyandiamide (210 °C). Consequently, the crystallization temperatures were set each to the melting point of calibration substance just before isothermal crystallization of PBT thin films. Finally the upper glass slide was removed and then the crystallized thin film was quenched onto a laboratory dish floating on the ice-cold water.

#### 2.1.2. Solution-cast crystallized film specimen

As same as the preparation of melt-crystallized film specimen, the 1.0 wt% and 0.1 wt% HFIP solutions were prepared for observations by POM and TEM, respectively. A solution

was dropped and spread on a carbon-coated glass slide, and the glass slide was covered with a Petri dish. To control the solvent-evaporation rate, some gap was applied between the laboratory desk and the rim of the dish and changed according to the evaporation rate at room temperature. Some of the specimens, which are prepared for morphological study by TEM, were ion-etched and/or stained with ruthenium tetroxide ( $\text{RuO}_4$ ).

### 2.2. Polarizing optical microscopy (POM)

The film specimens prepared from the 1.0 wt% solution of PBT were observed with a polarizing optical microscope ECLIPSE E600 POL (Nikon Co., Japan).

### 2.3. Transmission electron microscopy (TEM)

The film specimens prepared from the 0.1 wt% solution of PBT were mounted on copper grids for TEM according to the following procedures. The PBT thin films crystallized on the glass slides were coated with vapor-deposited carbon under vacuum for reinforcement. In order to calibrate the diffraction camera length, gold (Au) was vapor-deposited onto some of the films before carbon coating. A drop (a hemisphere 3–4 mm in diameter) of aqueous solution (ca. 25%) of polyacrylic acid (PAA) [12] was placed on the appropriate portion of the film specimen on the glass slide and hardened by drying for 1 day at room temperature. Hardened PAA with the film specimen was detached from the glass slide, and then the PAA was dissolved in water. Finally, the floating film specimen was mounted on a copper grid for TEM and dried under ambient condition.

Morphological observation and selected-area electron diffraction (SAED) of the resulting specimens were performed at room temperature with a transmission electron microscope JEM-200CS (JEOL Ltd., Japan) operated at an accelerating voltage of 200 kV.

## 3. Results and discussion

### 3.1. Three types of spherulites

As the results in the reports of Stein and Misra [7] and Roche et al. [8], three different types of PBT spherulites were formed depending on the crystallization conditions. Typical POM photographs of the three types of spherulites, taken with a sensitive color plate, are shown in Fig. 1. The crystallization conditions for Fig. 1(a)–(c) are as follows: (a) isothermally melt-crystallized at 210 °C for 24 h, (b) isothermally melt-crystallized at 163 °C for 20 h, and (c) solution-crystallized slowly by the solvent-evaporation method. Judging from the color-combination caused by the sensitive color plate, the spherulites shown in Fig. 1(a) are of usual-positive type (the first and third quadrants are blue-green and the others are yellow-orange), and the spherulites in Fig. 1(c) are of usual-negative type (the first and third quadrants are yellow-orange and the others are blue-green). (For

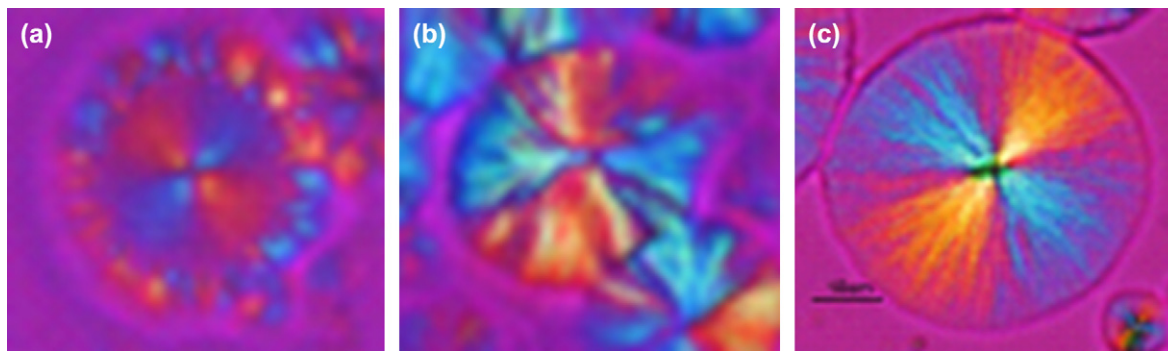


Fig. 1. Polarized light micrographs (taken with a sensitive color plate) of the PBT thin films crystallized under following conditions: (a) isothermally melt-crystallized at 210 °C for 24 h, (b) isothermally melt-crystallized at 163 °C for 20 h, and (c) solution-crystallized slowly by the solvent-evaporation method.

interpretation of the references to color in this figure citation, the reader is referred to the web version of this article.) The POM photograph (Fig. 1(a)) shows the clearly defined usual-positive type spherulite, although the utilized crystallization temperature is higher than those at which the formed spherulites did not show well-defined Maltese cross pattern [7] nor eight-arm cross pattern [9], as mentioned in Section 1. Therefore, as we know, this crystallization temperature of 210 °C is probably the highest one at which such a clearly defined usual-positive type of PBT spherulite is recognized, although the reason why in our experiment such a well-defined usual type was formed at higher crystallization temperature than those reported in Refs. [7,9] is not clarified at the present moment. Fig. 2 shows the three possible arrangements of optical ellipsoids within a spherulite, representing each birefringent crystal with the corresponding optical ellipsoid (refractive index ellipsoid) [13]. In the spherulite of usual-positive type, the direction of major axis of optical ellipsoid is coincident with the radial direction of spherulite as shown in Fig. 2(a), and in the usual-negative type, the direction of the major axis of optical ellipsoid coincides with the tangential direction of spherulite as shown in Fig. 2(c).

On the other hand, the spherulites shown in Fig. 1(b), in which the Maltese cross pattern is oriented at about 45° to the crossed polars, are of unusual type [14–16]. It is known

that if the optical ellipsoids are oriented at  $\theta$  to the radial direction of spherulite as shown in Fig. 2(b), the resulting Maltese cross pattern is oriented at  $\theta$  to the crossed polars [13]. Also when spherulites were grown under a rapid solution-crystallization condition by the solvent-evaporation method, the resulting spherulites were of unusual type. It should be emphasized here that our experimental results in Fig. 1 are not new, i.e., the results in Fig. 1 are nothing but a complete reproduction of the results reported by Stein and Misra [7] and Roche et al. [8].

### 3.2. Unusual type of spherulite

Fig. 3 shows bright-field defocus-contrast image of the thin films crystallized at 68 °C for 10 min. This crystallization condition is the one under which the unusual spherulites are formed. The SAED pattern obtained from the encircled area is set in the figure. Under this crystallization condition, growth of spherulite was stopped by collision of the spherulites and then the spherulites of irregular shape were formed. In the preliminary experiment for this crystallization condition, a typical SAED pattern obtained from the specimen area containing

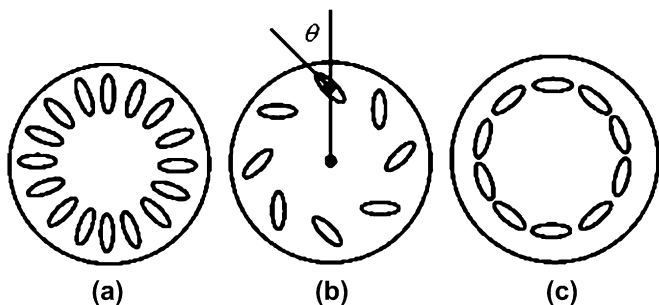


Fig. 2. Possible three arrangements of optical ellipsoids within a spherulite [13]: (a) spherically symmetric array with the major axis of ellipsoid parallel to the radius vector, (b) spherically symmetric array (a general model) with the major axis of ellipsoid tilted by an angle  $\theta$  from the radius vector, and (c) spherically symmetric array with the major axis of ellipsoid perpendicular to the radius vector.

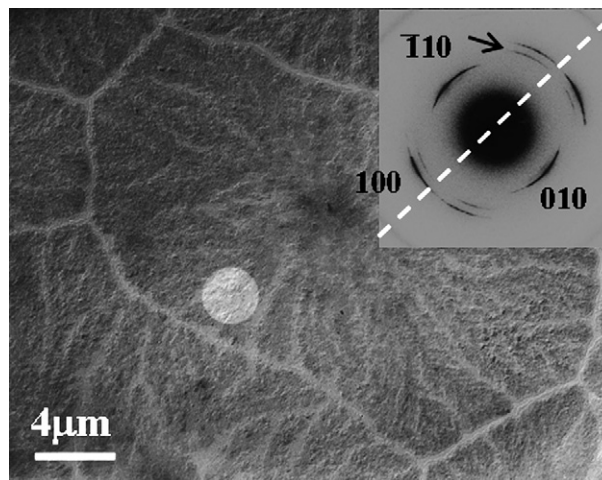


Fig. 3. Bright-field defocus-contrast image of the thin film melt-crystallized at 68 °C for 10 min, and the SAED pattern (inset) obtained from the encircled area.

approximately one irregular-shaped spherulite of the “unusual” type was characterized by several ringlike reflections.

By using the 111 reflection of Au as a reference, it is clarified that the SAED pattern shown in Fig. 3 was obtained only from the  $\alpha$ -modification. For indexing the reflections assigned to the  $\alpha$ -modification in this study, the unit cell parameters reported by Yokouchi et al. [3] were used (space group =  $P\bar{1} - Ci^1$ ;  $a = 0.495$  nm,  $b = 0.567$  nm,  $c$  (chain axis) = 1.295 nm,  $\alpha = 101.7^\circ$ ,  $\beta = 121.8^\circ$ ,  $\gamma = 99.9^\circ$ ). In order to know the growth direction of the spherulite, the SAED pattern in Fig. 3 was obtained with a rather small selected-area aperture (about 2.5  $\mu\text{m}$  in diameter) from the vicinity of the edge of the spherulite, because in this specimen area there are only lamellar crystals growing almost in the same direction (namely, in the radial direction of the spherulite). In the SAED pattern shown in Fig. 3, three kinds of reflections are recognized. Judging from the values of lattice spacing ( $d$ -spacing) for each of the reflections, these three kinds of reflections are assigned to the 010, 100, and 110 reflections (see the SAED pattern in Fig. 3). Here, it is known that the angle  $\varphi$  between the  $(h_1k_1l_1)$  and the  $(h_2k_2l_2)$  lattice planes equals the angle between their normals, as shown with the following equation:

$$\cos \varphi = \frac{\mathbf{h}_1 \cdot \mathbf{h}_2}{|\mathbf{h}_1| \cdot |\mathbf{h}_2|}, \quad (1)$$

where  $\mathbf{h}_1$  and  $\mathbf{h}_2$  are the reciprocal lattice vectors for the  $(h_1k_1l_1)$  and  $(h_2k_2l_2)$  planes, respectively. From Eq. (1), the theoretical value of the angle between the (010) and the (100) planes is calculated to be  $61.4^\circ$ , and that of the (010) and  $(\bar{1}10)$  planes is calculated to be  $73.0^\circ$ . Both theoretical angles are in good agreement with the ones estimated from the SAED pattern experimentally. Thus, from not only the lattice spacing but also the angle between lattice planes, it is confirmed that these three reflections in question are undoubtedly from the (010), (100), and  $(\bar{1}10)$  planes of PBT  $\alpha$ -modification crystal. Fig. 3, therefore, reveals that the 010 reflection appears in the direction approximately perpendicular to the growth direction

of spherulite (i.e., in the tangential direction of spherulite). This result means that the (010) plane is approximately parallel to the growth direction of spherulite (viz., to the radial direction of spherulite) and also parallel to the direction of the incident electron beam. It is also found that this SAED pattern corresponds to the [001] incidence of electron beam. This means that the arrangement of unit cell in one growing crystal ribbon in the unusual spherulite is the same as that in the PBT single crystal. Liu and Geil simulated a [001] ED pattern for the perfect PBT  $\alpha$ -modification crystal [6]. Briber and Thomas [11] investigated the single crystals made from random block copolymers of PBT and poly(tetramethylene ether glycol) and clarified that the long edges of the crystal lamellae are parallel to the (010) plane which is approximately parallel to the  $[\bar{2}10]^*$  reciprocal lattice direction. Fig. 4(a) is an SAED pattern obtained from PBT  $\alpha$ -modification single crystal obtained by us, and this pattern coincides well with the [001] ED pattern simulated by Liu et al. Fig. 4(b) is a schematic representation of the single crystal depicted by Briber and Thomas [11]. In this depiction (Fig. 4(b)), the thick rods correspond each to the projection of polymer chain in the unit cell of the  $\alpha$ -modification crystal onto the  $a^*-b^*$  plane (namely, onto the plane perpendicular to the chain axis ( $c$ -axis)). Comparing the SAED patterns of Figs. 3 and 4, it is found that SAED of unusual spherulite shows a (010)-twinlike pattern, although the intensity balance of reflections is not symmetrical. In this connection, the (010)-twin SAED patterns obtained from PBT crystals [6] and from PET ones [17] have been reported by Liu et al.

The growth direction of unusual spherulite should be parallel to the (010) plane, namely perpendicular to the  $[010]^*$  direction in the reciprocal lattice of  $\alpha$ -modification. Therefore, the  $[\bar{1}11]^*$  direction in the reciprocal lattice of  $\alpha$ -modification crystal, which was reported by Roche et al. [8] as a growth direction for unusual type spherulite, seems to be inappropriate in our case, because the theoretical value of the angle between the (010) and the  $(\bar{1}11)$  planes is calculated to be  $62.3^\circ$ . On the other hand, Roche et al. have proposed that the growth direction of the usual-negative type spherulite is  $[2\bar{1}0]^*$  in

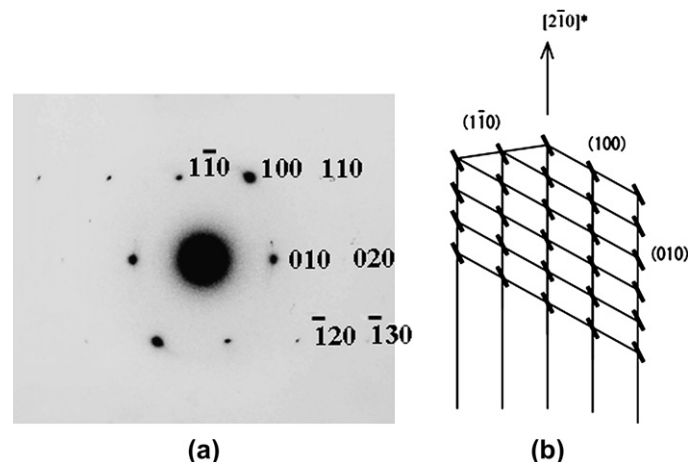


Fig. 4. (a) SAED pattern from a single crystal of PBT  $\alpha$ -modification. (b) Schematic illustration of a single crystal of PBT  $\alpha$ -modification [11].

the reciprocal lattice of  $\alpha$ -modification crystal. The theoretical value of the angle between the (010) and the ( $2\bar{1}0$ ) planes is calculated to be  $83.2^\circ$ . Although this value is not exactly  $90^\circ$ , the [ $2\bar{1}0$ ]\* can be taken as the preferred growth direction for the unusual type spherulite in our case. The reason, why the growth direction of unusual type spherulite determined by us disagrees with the one determined by Roche et al., has not been clarified. A major probable reason, however, can be that the preparation process of film specimen differs. In their case, the film specimens were prepared by the solution-cast crystallization with the solvent-evaporation method, while our film specimens were prepared by the isothermal melt-crystallization. In both types of crystallization processes, the unusual type spherulites are formed. However, it is very difficult to make a pure unusual type spherulite in the solution-cast crystallization, and then a mixed type spherulite of usual type and unusual type tends to be formed as mentioned in their report. Therefore, for TEM experiments, we chose the melt-crystallization as a specimen preparation method for the unusual type spherulite.

Fig. 5(a) shows a bright-field TEM image of the PBT thin film, which was prepared with the same condition as the one for the film specimen shown in Fig. 3 (namely, isothermally melt-crystallized at  $68^\circ\text{C}$  for 10 min). After crystallization, this film specimen was ion-etched and then stained with  $\text{RuO}_4$ . Ion-etching was applied first to remove the amorphous region which covers the whole film specimen and then  $\text{RuO}_4$  staining was applied to stain the remaining amorphous region. In Fig. 5, the bright portion corresponds to a crystalline region and the dark portion corresponds to an amorphous region. Fig. 5 reveals that an unusual spherulite is composed of many lathlike (ribbonlike) flat-on lamellar crystals which grow radially from the center of the spherulite. As mentioned above, in the unusual spherulite, the arrangement of unit cell within a lamella is the same as that in the single crystal which

is shown in Fig. 4(b). Because SAED shows the (010)-twinlike pattern (see Fig. 3), it is considered that the unusual spherulite contains two types of lamellae which are mirror images of each other as shown by the schematic illustrations of PBT  $\alpha$ -modification single crystals which are shown in Fig. 5. The growth direction [ $2\bar{1}0$ ]\* in the illustrations is suited to the radial direction of spherulite (namely, the growth direction of lathlike lamellar crystal). The boundary plane of these two illustrations is the (010) plane. In this stage, however, it is not clarified whether or not the (010) plane is a common plane between these two crystals, like a twin-crystal. Here, it should be emphasized that the percentage of both lamellar crystals is not 50/50.

The projection of a unit cell, in the unusual type spherulite, with one monomer onto the plane perpendicular to the viewing axis (namely, parallel to the specimen surface) is schematically depicted in Fig. 6, which was drawn with a software, “CrystalDesigner Ver.6.03 (Crystal Structure Design AS, Norway)”, in a personal computer. The direction of projection is parallel to the  $c$ -axis. It is known that in the  $\alpha$ -modification crystal the terephthalate residue is approximately planar, the plane of the residue being nearly parallel to the chain axis and also to the (100) lattice plane [3]. Thus, the silhouette of one monomer projected along the  $c$ -axis onto the  $a^*-b^*$  plane is well represented with an ellipse enclosing the monomer as depicted in Fig. 6. Furthermore, the optical anisotropy of one monomer in this projection should qualitatively be well demonstrated by using the ellipse. On the other hand, as shown in Fig. 2(b), Schultz simulated that, if the major axis of optical ellipsoids within a spherulite is tilted by an angle  $\theta$  from the radial direction of the spherulite, the resulting Maltese cross pattern is oriented at the angle  $\theta$  to the crossed polars [13].

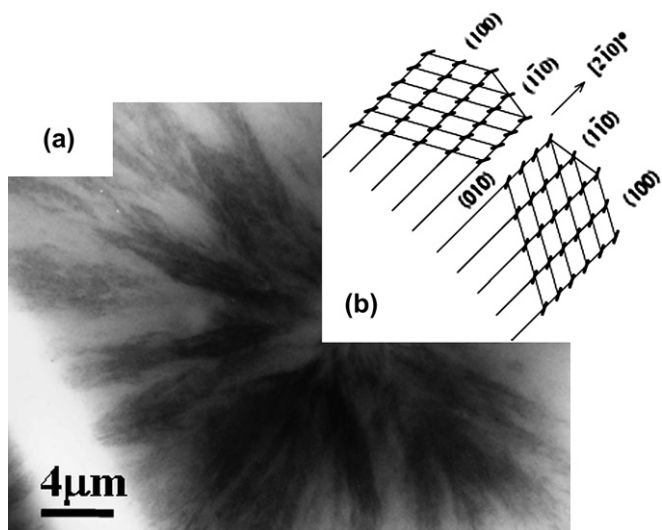


Fig. 5. (a) Bright-field image of the PBT thin film crystallized under same condition as Fig. 3 which was ion-etched and then  $\text{RuO}_4$ -stained. (b) Schematic illustration of two single crystals of PBT  $\alpha$ -modification, which are arranged to be like mirror images of each other.

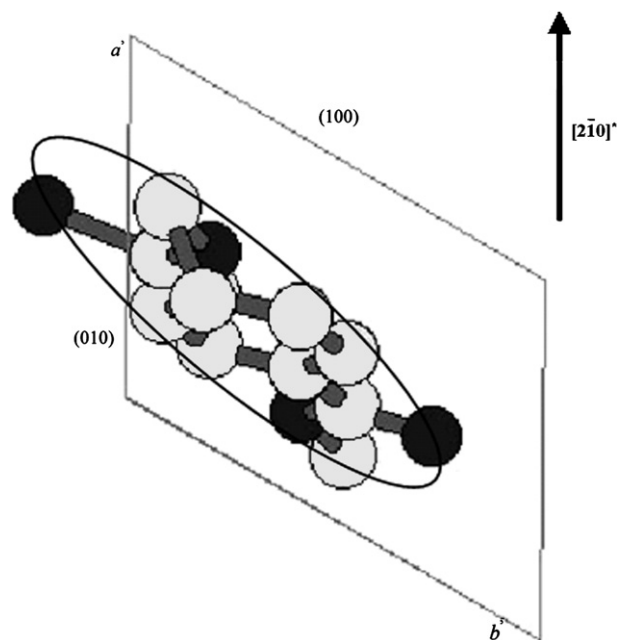


Fig. 6. Projection of a unit cell with one monomer unit within one lamellar crystal of the unusual type spherulite, viewed along the normal of specimen surface. Closed and open circles indicate oxygen and carbon atoms, respectively.

Therefore, it is speculated that the optical anisotropy expressed by the ellipse, the major axis of which leans by an angle of about  $60^\circ$  (namely, by the angle between (010) and (100) lattice planes) to the growth direction of lamella (namely, to the radial direction of the spherulite), determines the optical property of unusual type spherulite. From the schematic illustrations of unit cell arrangement shown in Fig. 5, which are in relation of mirror image with each other, you may misinterpret that both types of lamellar crystals exist at the same percentage (namely, 50/50) in a spherulite. If so, the effect due to the inclination of elliptic optical anisotropy will be compensated by these types each other, and then the optical property of unusual type will not appear under our consideration. Indeed, however, the SAED pattern in Fig. 3 shows that the abundance of both types of lamellar crystals, which are in relation of mirror image with each other, is not 50/50 at any time and one type predominates over the other in a spherulite.

### 3.3. Usual type of spherulites

#### 3.3.1. Usual-positive type

Fig. 7(a) shows a bright-field defocus-contrast TEM image of the thin film crystallized at  $210^\circ\text{C}$  for 24 h. This crystallization condition is the same as that for Fig. 1(a), that is to say, it is confirmed by the optical microscopy that the usual-positive type is formed under this crystallization condition. The corresponding SAED pattern obtained from the encircled area is set in the figure. The center of the spherulite is recognized, as indicated with the arrow in this image. Therefore the SAED pattern is obtained from a specimen area containing the lamellar crystals which grew effectively in the same direction. From both of the lattice spacing and the angle between lattice planes, the SAED pattern is characterized by the arc-shaped three reflections (010,  $1\bar{1}1$ , and 101) from the  $\alpha$ -modification.

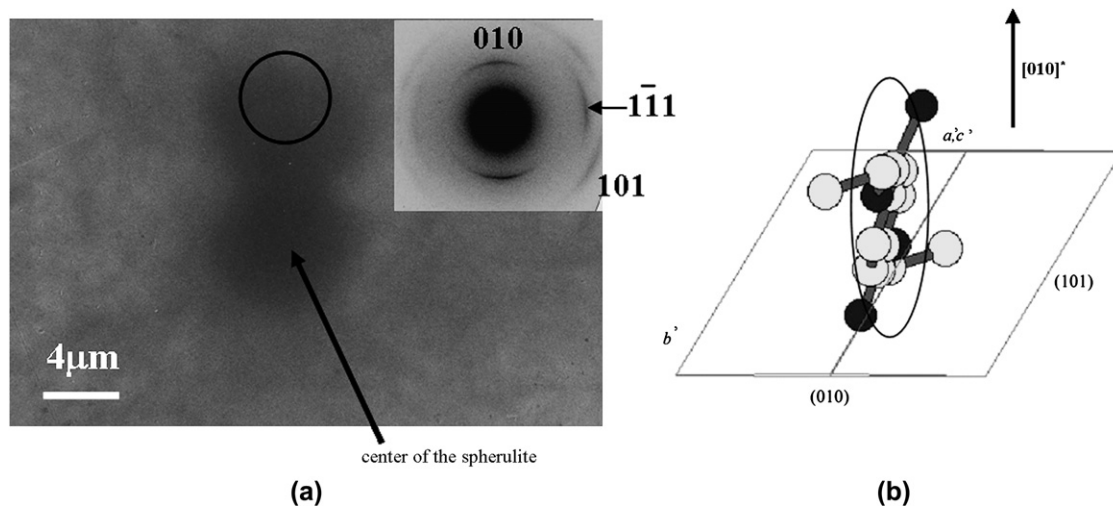


Fig. 7. (a) Bright-field defocus-contrast image of the thin film melt-crystallized at  $210^\circ\text{C}$  for 24 h and the SAED pattern (inset) obtained from the encircled area. The growth direction of the spherulite is approximately in the vertical direction of this image. (b) Projection of a unit cell with one monomer unit within one lamellar crystal of the usual-positive type spherulite, viewed along the normal of specimen surface. Closed and open circles indicate oxygen and carbon atoms, respectively.

This SAED pattern reveals that the incident electron beam direction is the  $[\bar{1}01]$  direction (namely, the pattern is called here as the  $[\bar{1}01]$  pattern). In contrast to the unusual spherulite, the 010 reflection appears approximately in the direction parallel to the growth direction of spherulite, although the (010) planes are preferentially oriented approximately parallel to the direction of the incident electron beam as in the case of unusual spherulite. Thus the arrangement of unit cell in the usual-positive spherulite can be related to that in the unusual spherulite by the following procedure: the arrangement of unit cell in the unusual spherulite is rotated by  $90^\circ$  around the  $c$ -axis of the unit cell and then rotated by about  $15^\circ$ , which is the angle between the (100) and the (101) lattice planes, around the  $[010]^*$  reciprocal lattice vector. The growth direction of usual-positive type spherulite is determined to be the  $[010]^*$  direction in the reciprocal lattice of  $\alpha$ -modification. The projection of a unit cell, in the usual-positive type spherulite, with one monomer along the  $[\bar{1}01]$  direction (namely, the incident electron beam) is schematically depicted in Fig. 7(b). The silhouette of one monomer in this projection can be well represented with an ellipse enclosing the monomer, and then it can be anticipated that optical anisotropy is qualitatively expressed well with this ellipse. This optical anisotropy expressed with the ellipse well corresponds to the refractive index ellipsoid shown in Fig. 2(a), that is to say, the direction of major axis of the ellipse is coincident with the radial direction of usual-positive type spherulite. Therefore, it is speculated that the optical anisotropy expressed by the ellipse determines the optical property of usual-positive type spherulite.

#### 3.3.2. Usual-negative type

Fig. 8(a) shows a bright-field defocus-contrast TEM image of the thin film which was crystallized slowly by a solvent-evaporation method. Under this crystallization condition,

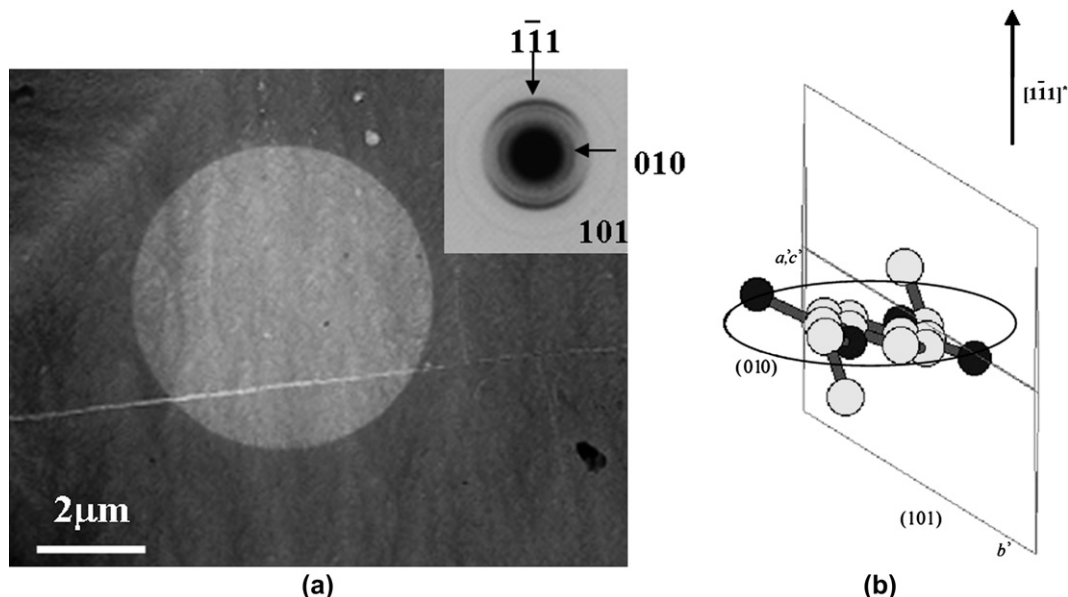


Fig. 8. (a) Bright-field defocus-contrast image of the thin film crystallized slowly by the solvent-evaporation method and the SAED pattern (inset) obtained from the encircled area. The growth direction of the spherulite is approximately in the vertical direction of this image. (b) Projection of a unit cell with one monomer unit within one lamellar crystal of the usual-negative type spherulite, viewed along the normal of specimen surface. Closed and open circles indicate oxygen and carbon atoms, respectively.

usual-negative type has to be formed. The SAED pattern was obtained from the vicinity of the edge of a spherulite. From both of the lattice spacing and the angle between lattice planes, the SAED pattern is characterized by the arc-shaped three reflections (010,  $1\bar{1}1$ , and 101) from the  $\alpha$ -modification, as the case of usual-positive type. It is noted, however, that each reflection appears at a position different by  $90^\circ$  from that for the corresponding reflection for the usual-positive type. Thus, it is found that the arrangement of unit cell in the usual-negative spherulite is related to that in the unusual spherulite by the following procedure: the arrangement of unit cell in the unusual spherulite is only rotated by about  $15^\circ$  around the  $[010]^*$  reciprocal lattice vector. This means that the incident electron beam direction is the same as in the case of one of the usual-positive types (namely, the  $[\bar{1}01]$  direction). On the other hand, the growth direction of the spherulite is the  $[1\bar{1}1]^*$  direction in the reciprocal lattice of  $\alpha$ -modification crystal. The projection of a unit cell, in the usual-negative type spherulite, with one monomer along the  $[\bar{1}01]$  direction is schematically depicted in Fig. 8(b). The silhouette of one monomer unit in this projection viewed along  $[\bar{1}01]$  can be well represented with an ellipse enclosing the monomer unit, and then it can be anticipated that optical anisotropy is qualitatively expressed well with the ellipse. Therefore, the direction of major axis of the optical ellipsoid is approximately perpendicular to the growth direction of lamella (namely, parallel to the tangential direction of the spherulite). This optical anisotropy expressed with the ellipse well corresponds to the refractive index ellipsoid shown in Fig. 2(c). Thus, it is speculated that, in the usual-negative type, the optical anisotropy expressed with this ellipse determines the optical property of spherulite.

#### 4. Conclusion

Three kinds of thin film specimens, each of which containing one of the three types of two-dimensional PBT spherulites (i: usual-positive type, ii: usual-negative type, and iii: unusual type), were prepared. By SAED, it was confirmed that all these kinds of spherulites are made up of only the  $\alpha$ -modification crystals. The SAED experiments for a specific specimen area containing only the lamellar crystals, which grew effectively in the same direction, clarified that the growth directions for usual-positive type, usual-negative type, and unusual type are the  $[010]^*$ ,  $[1\bar{1}1]^*$ , and  $[2\bar{1}0]^*$  directions in the reciprocal lattice, respectively. Furthermore, the arrangement of unit cell in each type of the spherulites was determined, by the SAED experiments. The structural origins, each of which determining the optical property of the corresponding two-dimensional PBT spherulite, can be well attributed to the elliptical shape and its major-axis direction of each silhouette of one monomer projected along the viewing axis (namely, to the normal of the specimen surface), that is to say, one direction of the major axis of elliptical silhouette corresponds to one of the major axes of optical ellipsoid in the well known refractive index ellipsoid model for each type of spherulites.

#### Acknowledgments

This work was supported by a Grant-in-Aid for Scientific Research (C) (2), No. 16550174, from Japan Society for the Promotion of Science (JSPS) to which M.T. wishes to express his gratitude.

**References**

- [1] Gilbert M, Hybart FJ. *Polymer* 1972;13:327–32.
- [2] Gilbert M, Hybart FJ. *Polymer* 1974;15:408–12.
- [3] Yokouchi M, Sakakibara Y, Chatani Y, Tadokoro H, Tanaka T, Yoda K. *Macromolecules* 1976;9:266–73.
- [4] Hall IH, Pass MG. *Polymer* 1976;17:807–16.
- [5] Desborough IJ, Hall IH. *Polymer* 1977;18:825–30.
- [6] Liu J, Geil PH. *J Macromol Sci Phys* 1997;B36:263–80.
- [7] Stein RS, Misra A. *J Polym Sci Polym Phys Ed* 1980;18:327–42.
- [8] Roche EJ, Stein RS, Thomas EL. *J Polym Sci Polym Phys Ed* 1980;18:1145–58.
- [9] Lorenzo MLD, Righetti MC. *Polym Eng Sci* 2003;43:1889–94.
- [10] Briber RM, Thomas EL. *Polymer* 1985;26:8–16.
- [11] Briber RM, Thomas EL. *Polymer* 1986;27:66–70.
- [12] Novillo FA, Fujita M, Tsuji M, Kohjiya S. *Sen-i Gakkaishi* 1998;54:544–9.
- [13] Schultz JM. *Polymer crystallization – the development of crystalline order in thermoplastic polymers*. Oxford University Press; 2001 [chapter 4].
- [14] Rhodes MB, Stein RS. *J Polym Sci* 1962;62:S84–8.
- [15] Rhodes MB, Stein RS. *Polym Lett* 1963;1:663–7.
- [16] Rhodes MB, Stein RS. *J Appl Phys* 1968;39:4903–9.
- [17] Liu J, Geil PH. *J Macromol Sci Phys* 1997;B36:61–85.